European Journal of Pharmaceutical Sciences 128 (2019) 270–278

Contents lists available at ScienceDirect

European Journal of Pharmaceutical Sciences

journal homepage: www.elsevier.com/locate/ejps

Synthesis and characterization of nanostructured lipid-poloxamer organogels for enhanced skin local anesthesia

Aryane Alves Vigato[a], Samyr Machado Querobino[a], Naially Cardoso de Faria[a], Andréa Carolina Pinheiro de Freitas[b], Gislaine Ricci Leonardi[b], Eneida de Paula[c], Cíntia Maria Saia Cereda[d], Giovana Radomille Tófoli[d], Daniele Ribeiro de Araujo[a,*]

[a] Human and Natural Sciences Center, Federal University of ABC, Santo André, SP, Brazil
[b] Faculty of Pharmaceutical Sciences, State University of Campinas, Campinas, SP, Brazil
[c] Department of Biochemistry, State University of Campinas, Campinas, SP, Brazil
[d] São Leopoldo Mandic Research Unit, São Leopoldo Mandic Faculty, Campinas, SP, Brazil

ARTICLE INFO

Keywords:
Organogels
Poloxamer
Lanolin
Local anesthesia
Skin permeation

ABSTRACT

The aim of this study was to synthesize a novel drug delivery system using organogels (ORGs) and characterize its physicochemical properties, in vitro and ex vivo permeation abilities, cytotoxicity and in vivo local anesthetic effects. The ORG formulations contained a mixture of oleic acid-lanolin (OA-LAN), poloxamer (PL407), and the commonly used local anesthetic lidocaine (LDC). The main focus was to evaluate the impact of LAN and PL407 concentrations on the ORG structural features and their biopharmaceutical performance. Results revealed that LDC, OA, and LAN incorporation separately shifted the systems transitions phase temperatures and modified the elastic/viscous moduli relationships ($G'/G'' = \sim 15\times$). Additionally, the formulation with the highest concentrations of LAN and PL407 reduced the LDC flux from ~17 to 12 $\mu g \cdot cm^{-2} \cdot h^{-1}$ and the permeability coefficients from 1.2 to 0.62 $cm \cdot h^{-1}$ through *ex vivo* skin. *In vivo* pharmacological evaluation showed that the ORG-based drug delivery system presented low cytotoxicity, increased and prolonged the local anesthetic effects compared to commercial alternatives. The data from this study indicate that ORG represent a promising new approach to effectively enhance the topical administration of local anesthetics.

1. Introduction

Local anesthesia is one of the most used therapeutic practices for minimizing anxiety, pain, and discomfort during surgical dermatology procedures. The main formulations are available as creams and gels. However, these often do not provide adequate analgesic effects at the site of injection or surgical procedure. Toward overcoming this limitation, new pharmaceutical formulations are being developed that safely prolong and enhance the anesthetic effect at the site of administration (Park and Sharon, 2017).

The topical administration of local anesthetics (LAs) is hampered by the inability of traditional analgesic agents to effectively penetrate the skin. The stratum corneum is the main barrier preventing permeation due to its particular lipid composition (free fatty acids, phospholipids, cholesterol, cholesterol sulfate, and ceramides). Several recent publications describe strategies to overcome this limitation by developing colloidal systems such as liposomes, niosomes, micelles, nanocapsules, nanoparticles (polymeric, solid lipids), emulsions, hydrogels, and organogels (de Araujo et al., 2013; Alsaab et al., 2016).

Among the various systems investigated for maximizing skin delivery, one of the most promising involve poloxamers (PLs), which are triblock copolymers composed of a central hydrophobic chain of polypropylene oxide (PPO) and two polyethylene oxide (PEO) hydrophilic chains (Dumortier et al., 2006). The main advantage of using PLs in pharmaceutical formulations is their ability to self-assemble into micelles under nearly physiological temperatures (Patel et al., 2009; Oshiro et al., 2014). In response to temperature and concentration, the PPO dehydrates and aggregates, while the PEO remains hydrated, thereby forming the micellar core and shell, respectively, even in PL binary systems (Lee et al., 2010). Subsequently, these micelles self-assemble into a three-dimensional network, forming thermoreversible hydrogels that can be used as matrices to carry nanoparticles and, importantly, with an aqueous phase for organogels (ORGs).

ORGs are semi-solid systems in which an organic liquid phase is

* Corresponding author at: Centro de Ciências Naturais e Humanas, Universidade Federal do ABC, UFABC, Av. dos Estados 5001, Bloco A, Torre 3, Lab 503-3, Bairro Bangú, Santo André, SP CEP 090210-580, Brazil.
E-mail address: daniele.araujo@ufabc.edu.br (D.R. de Araujo).

https://doi.org/10.1016/j.ejps.2018.12.009
Received 31 August 2018; Received in revised form 21 November 2018; Accepted 11 December 2018
Available online 12 December 2018
0928-0987/

Table 1
Formulations components for different ORG containing lidocaine (LDC).

Formulations	Aqueous phase (AP)	Organic phase (OP)	
	Poloxamer 407 (PL 407, %wt)	Oleic acid (OA) organic solvent	Lanolin (LAN, %wt)
OA-PL_{407} (20)	20	OA	–
OA-PL_{407}-LAN (20-0.5)		OA	0.5
OA-PL_{407}-LAN (20-1)		OA	1
OA-PL_{407}-LAN (20-3)		OA	3
OA-PL_{407} (30)	30	OA	–
OA-PL_{407}-LAN (30-0.5)		OA	0.5
OA-PL_{407}-LAN (30-1)		OA	1
OA-PL_{407}-LAN (30-3)		OA	3

Organic:Aqueous phase ratio of 1:4 (OP:AP, v/v) and LDC final concentration was 2%.

immobilized by a three-dimensional network composed of a self-organizing, gel-like material. Despite their considerable liquid composition, ORGs exhibit the rheological behavior of a solid material, thus enabling the delivery of a variety of different molecules; as such, ORGs can serve as vehicles capable of modulating drug permeation across the skin (Almeida et al., 2012; Elnaggar et al., 2014; Vintiloiu and Leroux, 2008). PL-based ORGs can effectively disperse hydrophobic drugs by combining the three-dimensional structure of PL with organic compounds such as isopropyl palmitate (Jatav and Ramteke, 2015), isopropyl myristate (Jantharaprapap and Stagni, 2007), lecithin (Belgamwar et al., 2008) and other lipid components, such as lanolin (Jantharaprapap and Stagni, 2007). Different skin delivery systems for LAs have been reported, including solid, polymeric, and hybrid nanoparticles (You et al., 2017; Zhang et al., 2016; Wang et al., 2016), microemulsions (Zhang and Michniak-Kohn, 2011), and PL-based hydrogels (Akkari et al., 2016). Among these, ORGs are particularly promising because they can solubilize an LA in either base or salt form due to their organic/aqueous nature. While research on alternative delivery systems for LAs such as lidocaine (LDC) (Sallam et al., 2015; Bakonyi et al., 2018) is limited, this drug was chosen for this study due to its widespread clinical use.

In this context, the aim of this study was to synthesize and evaluate various ORG formulations based on the mixture of oleic acid-lanolin (OA-LAN) and PL407, toward developing an optimized topical delivery system for LDC. Specifically, we investigated the influence of LAN and PL407 concentrations on the physicochemical properties of ORGs, including calorimetric, morphological, and rheological characterization, followed by cytotoxicity, functional evaluation using in vitro and ex vivo permeation studies and an in vivo model.

2. Materials and methods

2.1. Chemicals and reagents

PL407 (Pluronic® F-127), OA, LAN, and LDC were purchased from Sigma–Aldrich (St. Louis, MO, USA). All chemicals and solvents were analytical grade. Commercial gel (CG, composed of lidocaine hydrochloride 2%, hietelose, methylparaben, sodium hydroxide, water), Commercial cream (CC, lidocaine 4%, benzyl alcohol, carbomer 980, cholesterol, soy lecithin, polysorbate 80, propylene glycol, trolamine, alfatocopherol acetate and water).

2.2. High-performance liquid chromatography (HPLC)

LDC levels were quantified using an HPLC system (Ultimate 3000, Chromeleon 7.2 software, Thermo Fisher Scientific, Waltham, USA) with a gradient pump, DAD detector, and C18 column (150 × 4.6 mm, 5 µm; Phenomenex, USA). LDC samples were analyzed at 210 nm with a 0.5 mL/min flow rate at 25 °C. The mobile phase was a mixture of acetonitrile and phosphate-buffered solution (60:40). The drug retention time was 2.5 min. This method was chosen based on recommendations from the International Conference on Harmonization and the results represent three experiments performed in triplicate. The limits of detection (LD) and quantification (LQ) were determined from a standard curve of LDC at 10, 15, 30, 40, 50, and 60 µg/mL. The LD and LQ values were 3.24 and 9.82 µg/mL, respectively. The LDC concentration was determined using the equation $y = 0.634 * x \pm 0.42$. The correlation coefficient (R^2) value was 0.995.

2.3. ORG preparation

The ORG samples were prepared according to published methods with only minor modifications (Boddu et al., 2014). Briefly, the organic phase (OP) was prepared using 2 mL of OA alone or combined with different concentrations of LAN (0.5, 1, and 3% wt). LDC (100 mg·mL^{-1}) was added to the OP and stirred magnetically (350 rpm, at 25 °C) until completely dissolved (2% wt final concentration). The aqueous phase (AP) was prepared by dissolving the appropriate amount of PL407 (20 or 30% wt) in HPLC-grade water in an ice bath with continuous stirring (350 rpm) until the solution became transparent. The OP was then added to the AP (1:4 v/v) and homogenized, under magnetic stirring (350 rpm) until a homogeneous gel was obtained. Finally, sodium benzoate (0.25% wt) was added to all of the formulations as a preservative. The composition of all eight ORG sample formulations is presented in Table 1.

2.4. Organoleptic characterization, drug content, and pH determination

The ORG formulations were initially assessed by manual inspection of color, odor, phase separation, and precipitate formation. The pH of every ORG was recorded after allowing the probe to equilibrate in each gel. The drug content was determined by weighing an exact amount (equivalent to 0.05 g) of ORG into a test tube to which 10 ml of acetonitrile:water (70:30 v/v) was added. This mixture was sonicated for approximately 20 min in an ultrasonic bath sonicator and then filtered (nylon syringe filter, 0.22-µm pore). The resulting solution was diluted in acetonitrile:water (70:30 v/v) and analyzed by HPLC to determine the LDC concentration. Drug content was expressed as a percentage.

2.5. Morphological analysis

Morphological analysis of the ORGs was performed using optical, polarized light, and scanning electron microscopy (OM, PLM, and SEM, respectively). For the OM and PLM analysis, aliquots of each sample were deposited in a thin layer onto a glass microscope slide and then covered with coverslips. The slides were then analyzed between crossed polarizers (PLM) using an optical microscope (Axio Lab A1 with AxioCam ICc 5, Carl Zeiss, Germany) to detect anisotropy. SEM analyses were performed on a JEOL JSM 6000 microscope (JEOL, Peabody, USA). A thin film of the ORG was dried onto a glass slide in a desiccator for 24 h at room temperature. The resulting dry powder was placed on a metal stub with carbon adhesive tape and coated with platinum/

palladium alloy under vacuum pressure. The equipment was operated at 10 kV and images were acquired under 440× magnification.

2.6. Differential scanning calorimetry (DSC) analysis

The DSC experiments were carried out using a Netzsch DSC Polyma calorimeter (Netzsch, Selb, Germany). 20 mg of ORG was placed in the sealed aluminum pan. Samples were analyzed across three thermal cycles (heating-cooling-heating) from 0 to 50 °C at a rate of 5 °C/min. Thermogram data were presented as heat flux (J/g) versus temperature (°C). An empty pan was used as the reference.

2.7. Rheological assays

Rheological analyses were performed using an oscillatory Kinexus rheometer (Malvern Instruments Ltd., UK) with cone-plate geometry. To determine the sol-gel transition temperatures ($T_{sol-gel}$), the frequency was set at 1 Hz and the temperature ranged from 10 to 50 °C. Subsequently, the temperature was kept at 32.5 °C and the samples were analyzed under a frequency sweep from 0.1 to 10 Hz. These oscillatory measurements were used to obtain the elastic modulus (G′), viscous modulus (G″), and viscosity (η*) for each ORG formulation immediately and until 90 days after preparation, in order to evaluate the formulations stability. Data were analyzed with the rSpace for Kinexus® software.

2.8. In vitro and ex vivo permeation studies

The *in vitro* permeation studies were performed using vertical Franz-type diffusion cells (Vision Microette Plus; Hanson Research, Chatsworth, CA, USA). This transdermal diffusion test model involves two compartments, a donor (1.72 cm^2 permeation area) and receptor (7 ml) region, separated by a synthetic membrane (Strat-M® membranes, 25-mm discs, Millipore Co., USA, ultrafiltration membrane, 325 µm thick) (Uchida et al., 2015; Sallam et al., 2015; Kaur et al., 2018). ORG formulations (0.3 g/cm^2) were applied to the donor compartment (in contact with the upper surface of the Strat-M® membrane). The receptor compartment was filled with 7 mL of pH 7.4 HEPES (5 mM) buffered saline (154 mM) solution and stirred magnetically (350 rpm, for 8 h) at 32.5 ± 0.5 °C.

The ex vivo permeation studies were performed using the same vertical Franz-type diffusion cells but with a 0.64 cm^2 donor permeation area and a 4.5 mL receptor volume. The two compartments were separated by full-thickness skin from a pig's ear obtained from a slaughter-house that would've otherwise been discarded. The animal protocol was approved by the UFABC Institutional Animal Care and Use Committee (#8719010318). The tissue was sliced into 0.45-mm sections using a 75 mm dermatome (Nouvag, Rorschach, Switzerland). The skin was then excised from the underlying cartilage using a scalpel and stored at −20 °C until use.

The ex vivo permeation experiments were performed under the same conditions described for the in vitro ones. For both assays, aliquots from the receptor compartment were collected ever 30 min for 8 h and then analyzed by HPLC. All experiments were performed in triplicate. The cumulative amount of LDC that permeated into the receptor compartment was expressed as µg·cm^{-2} and results were plotted as a function of time (h).

Drug flux values were obtained from the slope of the curve over the 8-h period. Data were analyzed according to the following equation (Eq. (1)):

$$J = P \cdot Cd \quad (1)$$

where J (µg·cm^{-2}·h^{-1}) is the drug flux across the membrane or skin, P (cm·h^{-1}) is the permeability coefficient, and Cd (µg·cm^{-3}) is the drug concentration in the donor compartment. The lag time was calculated by extrapolating a straight line to time axis (de Araujo et al., 2010).

2.9. In vitro cytotoxicity and in vivo pharmacological assays

HaCaT cells line, human epidermal keratinocytes (Thermo Fisher Sci. Waltham, Massachusetts, USA), was used for the in vitro experiments. Cells were cultured, in 96-well plates for 48 h (2.104 cells/well), in Dubelcco's Modified Eagle Medium (DMEM; Gibco Laboratories, Grand Island, NY, USA) supplemented with 10% (v/v) fetal bovine serum (pH 7.2–7.4), humidified atmosphere at 37 °C and 5% CO_2 and 100 µg·mL^{-1} of penicillin/streptomycin cells. Before cells treatment, ORG formulations OA-PL407 (20), OA-PL407 (30), OA-PL407-LAN (20-3), OA-PL407-LAN (30-3) were diluted in culture medium until the final concentration range from 10 mg·mL^{-1} to 0.16 mg·mL^{-1} and 200 µL from each solution were then incubated with cells for 24 h. After that, 100 µL of MTT solution (5 mg·mL^{-1}, in phosphate buffered saline) was added to each well and cells treated for 4 h. Then, MTT solution was removed, 50 µL of DMSO was added to each well for 10 min, and the absorbance measured at 570 nm. As negative control, non-cytotoxic, cells were treated only with DMEM at the same volume used for formulations treatment.

For pharmacological assays, adult male Swiss mice (30–35 g) were obtained from CEMIB-UNICAMP (Centro de Bioterismo, State University of Campinas-UNICAMP, Campinas, São Paulo, Brazil). The animal protocol was approved by UNICAMP Institutional Animal Care and Use Committee, in accordance with the Guide for the Care and Use of Laboratory Animals (#4859-1/2018). Pharmacological efficacy was evaluated using the tail flick test. The ORG formulations were compared to two commercial formulations (Commercial gel, CG; Commercial cream, CC; with 2 and 4% LDC, respectively). For baseline determination (i.e. a typical stimulus response), the animal was placed in a horizontal restraint support and a portion of the tail (2 cm from the tip) was exposed to an analgesimeter with a projector lamp (55 ± 1 °C) connected to a control switch and a timer. The time interval between temperature exposure and tail flick was recorded (in s) and referred to as latency time. A cut-off time of 10 s was used to prevent any thermal injury to the tail tissue. Baseline latency times were recorded for all animals prior to the experimental treatment.

Formulations (0.1 g) were gently applied to the distal portion of the tail (2 cm from the tip). The experimental evaluation was initiated 30 min after sample application and then repeated until 6 h after the initial treatment. Results were expressed as percentage of animals with analgesic effects, duration of the analgesic effect (h), and area under the efficacy curve ($AUEC_{0-6h}$) for each group.

2.10. Statistical analyses

All data were presented as mean ± standard deviation. A one-way analysis of variance (ANOVA) was performed for between-group comparisons followed by the Tukey-Kramer post-hoc test for multiple comparisons. Data were analyzed using the Origin 6.0 software (Microcal™ Software, Inc., Northampton, MA, USA). Statistically significant differences were defined as $p < 0.05$.

3. Results and discussion

3.1. Organoleptic, pH, drug content and morphological characterization

The ORG formulations were opaque and slightly yellow, which was different from hydrogels prepared as aqueous phases (Fig. 1A–C). There were no particulate materials nor any phase separation. As expected, the SEM analyses confirmed the typical arrangement of PL407 hydrogel into flat layers (Fig. 1A), similar to those described by Akkari et al. (2016). In contrast to the traditional morphological pattern of PL407, the ORG formulations (Fig. 1B–E) had an amorphous appearance with wrinkled surfaces, resulting from the incorporation of the organic phase into the aqueous phase. OM revealed that the ORG formulations were morphologically homogeneous and continuous (Fig. 1F–I).

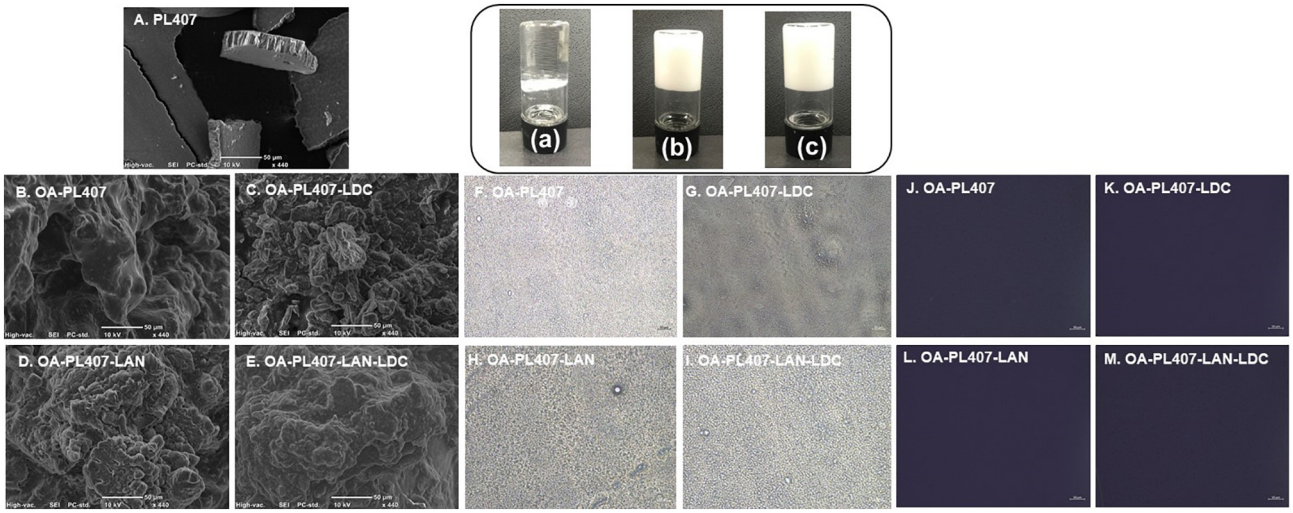

Fig. 1. Micrographies of OA-PL organogels obtained from Scanning Electron Microscopy (A–E), Optical (F–I) and Polarized Light Microscopy (J–M). (a) PL407 hydrogel, (b) OA-PL_{407} and (c) OA-PL_{407}-LAN.

Furthermore, neither birefringence nor anisotropy were detected using PLM (Fig. 1J–M), indicating that the LDC and LAN were homogeneously incorporated into the gels. The pH values of the ORG samples containing LAN and LDC were around 4.8 and 6.4, respectively, in agreement with other ORGs systems prepared with ricinoleic acid and PL407 concentrations from 8 to 16% (Boddu et al., 2015). The LDC content was quantified as 95.31 ± 6.85% and 97.31 ± 5.93% for OA-PL_{407} and OA-PL_{407}-LAN, respectively, which confirmed that the drug was homogeneously distributed throughout the ORGs.

3.2. DSC analysis

All of the ORG formulations were analyzed by DSC to determine their initial (T_{onset}), peak (T_{peak}), and final (T_{endset}) phase transition temperatures in addition to the enthalpy change (ΔH) of each phase transition. These results are presented in Table 2.

These analyses revealed shifts in the phase-transition temperature values in response to LDC and LAN incorporation. The formulation OA-PL_{407} exhibited similar T_{onset}, T_{peak}, and T_{endset} at both 20 and 30% PL407. However, after LDC incorporation, T_{peak} shifted from 10.1 °C to 12.6 °C, for OA-PL_{407} (20) and OA-PL_{407} (30), respectively. This shift reflects the drug's interference with the phase transition process, possibly due to the dispersion of the LDC base into the organic phase. In fact, LDC addition to the organic phase of the ORGs reduced the ΔH from 0.99 to 0.41 $J{\cdot}g^{-1}$ for the OA-PL_{407} (30) system. These results suggest that the LDC molecules enthalpically favor the PL407 micellization process, as has been described for other hydrophobic drugs (Sharma et al., 2008; Esposito et al., 2018).

Comparisons among the OA-PL_{407} (20) systems containing LAN revealed reductions in T_{onset} values at 1 and 3% LAN. For OA-PL_{407} (30), the different LAN concentrations did not significantly alter either the T_{onset} or T_{peak} values, which can be attributed to the self-assembled micelle-micelle networks and the increased structural organization generated under high PL407 concentrations. Additionally, the presence of LAN in the formulations increased the ΔH values compared to OA-PL_{407} systems without LAN. These effects can be attributed to LAN long carbon chains (given their composition of aliphatic mono-alcohols, sterols, non-hydroxy and hydroxy fatty acids, from C8 to C41) (Sengupta and Behera, 2014) and their interactions with the non-polar polypropylene glycol central blocks from the PL407 molecules, which can strongly impact the PL micellization process. Also worthy of consideration are the potential hydrophobic interactions between the

Table 2
Temperatures (T) and enthalpy variation (ΔH) relative to the phase transition for OA-PL_{407} organogels before and after 0.5; 1 or 3% LAN incorporation.

Formulations		Additives	T_{onset} (°C)	T_{peak} (°C)	T_{endset} (°C)	ΔH ($J{\cdot}g^{-1}$)
PL407 hydrogel (20%)		–	10.0	15.1	20.1	0.99
PL407 hydrogel (30%)		–	9.8	13.5	23.9	0.32
20%	OA-PL_{407}	–	10.1	12.1	14.2	0.3
		LDC	8.1	10.1	13.4	0.4
		LAN 0.5%	9.6	12.7	15.5	2.3
		LAN 0.5% - LDC	7.0	9.8	13.7	0.9
		LAN 1%	8.1	12.8	16.2	5.7
		LAN 1% - LDC	6.3	9.9	14.3	0.9
		LAN 3%	7.0	12.5	15.6	6.4
		LAN 3% - LDC	7.1	9.8	13.1	0.5
30%	OA-PL_{407}	–	9.2	11.7	14.6	1.0
		LDC	10.4	12.6	15	0.4
		LAN 0.5%	8.3	13.4	17	9.0
		LAN 0.5% - LDC	5.4	12.5	16.5	11.5
		LAN 1%	10.6	12.9	15.9	1.6
		LAN 1% - LDC	5.2	12.3	16.4	12.6
		LAN 3%	10	13.7	17.8	6.5
		LAN 3% - LDC	5.3	12.7	16.6	13.5

Tonset, Tpeak and Tendset are the initial, peak and final phase transitions temperatures, respectively. OA - oleic acid; LAN - lanolin; PL_{407} - poloxamer 407; LDC - lidocaine.

carbon chains of OA (C18) and LAN. Taken together, the presence of each component contributes to complex molecular interactions in the organic phase.

The large temperature range between T_{onset} and T_{endset} obtained for OA-PL_{407} (20) and OA-PL_{407} (30), when compared to the OA-PL_{407} and OA-PL_{407}-LAN systems (Table 2), may indicate that different endothermic processes are capable to promote changes on formulations structural organization. This explanation is supported by the reduced intervals between T_{onset} and T_{endset} in the presence of OA and/or LAN.

3.3. Rheological assays

The rheological parameters obtained for a formulation are dependent on the physicochemical properties and compatibility among the components, the nature of the encapsulated substances, and the composition of the organic phase (Sagiri et al., 2015; Sagiri et al., 2014; Dassanayake et al., 2012). Rheological studies can be used to examine differences on elasticity and viscosity is well-known properties related to the material's behavior as a solid and a liquid. Despite their predominantly liquid composition, ORGs display the rheological behavior usually associated with solids, i.e. a larger elastic modulus (G′) relative to the viscous modulus (G″). Additionally, $T_{sol\text{-}gel}$ is one of the most important parameters for estimating the influence of different components on ORG structural organization and their compatibility.

The OA-PL_{407} systems were analyzed according to variations in PL407 concentration (20 or 30%), LAN concentration (0.5, 1, and 3%) as well as the LDC. Figs. 2 and 3 contain the rheograms used for $T_{sol\text{-}gel}$ determination and data from the frequency sweep analysis, respectively, for the 20% PL407-based systems.

For the OA-PL_{407} systems with 20% PL407, rheological analysis showed similar $T_{sol\text{-}gel}$ values ranging from 12 to 14 °C in the presence of LAN and LDC. On the other hand, OA-PL_{407} systems with 30% PL407 showed no shifts after LAN and LDC incorporation (Table 3) with $T_{sol\text{-}gel}$ values < 8 °C due to the higher PL407 concentration.

All ORG formulations exhibited viscoelastic behavior and were stable under temperature variation, showing G′ > G″ values. However, the presence of LAN reduced the G′/G″ relationships (from ~30 to 14) for both the 20 and 30% PL407 formulations. Similar rheological behaviors were observed for the OA-PL_{407}-LAN-LDC formulations (Table 3).

LDC incorporation into the OA-PL_{407} system increased the G′ and η* values (Table 3), which is indicative of a decrease in viscosity. This effect can be attributed to the interference introduced by the LDC molecules in the gel three-dimensional structure formation, conferring it greater organization (Mady et al., 2016). In fact, considering that the LDC base has a high partition on organic phases, it is possible that these molecules could be interacting with both organic phase and the hydrophobic propylene glycol chains in the PL micellar core, as has been reported for PL-based binary systems containing LDC (Nascimento et al., 2018). In contrast, LAN addition to the organic phase decreased the G′/G″ ratios and the η* values, indicating a possible loss of the three-dimensional ORG network caused by the long hydrophobic chains of the LAN (Sharma et al., 2018); thus, these data corroborate the calorimetric results, discussed before.

The frequency sweep analysis revealed that the values for both G′ and G″ were not significantly affected by increasing the applied frequency. Since G′ describes a materials elasticity, higher G′ relative to G″ values correspond to greater structural organization within a system. In addition, rheological analysis also showed high G′ > G″ for ORGs until 90 days after preparation (Fig. 4), where no differences were observed between recent and 90 days rheological profiles, highlighting the formulations structural stability. This feature is relevant for a topical treatment because it relays whether the formulation allows for some deformation without the loss of gel structure and stability.

3.4. In vitro and ex vivo permeation studies

Permeation assays across the Strat-M® artificial membranes (Fig. 5A) and skin sections (Fig. 5B) were performed with every OA-PL_{407} formulation (20 and 30% PL407), with and without LAN (0.5, 1, and 3%). All experiments were made in infinity dose conditions and the results are summarized in Table 4.

Permeation profiles across Strat-M® showed increased cumulative drug concentrations during the experiment (8 h) for all formulations. However, differences on drug permeated concentrations were revealed by comparisons among OA-PL_{407} ORG containing 20 and 30% PL407 clearly segregated into two well-defined groups (particularly 4 h post-treatment) according to polymer concentration in the aqueous phase.

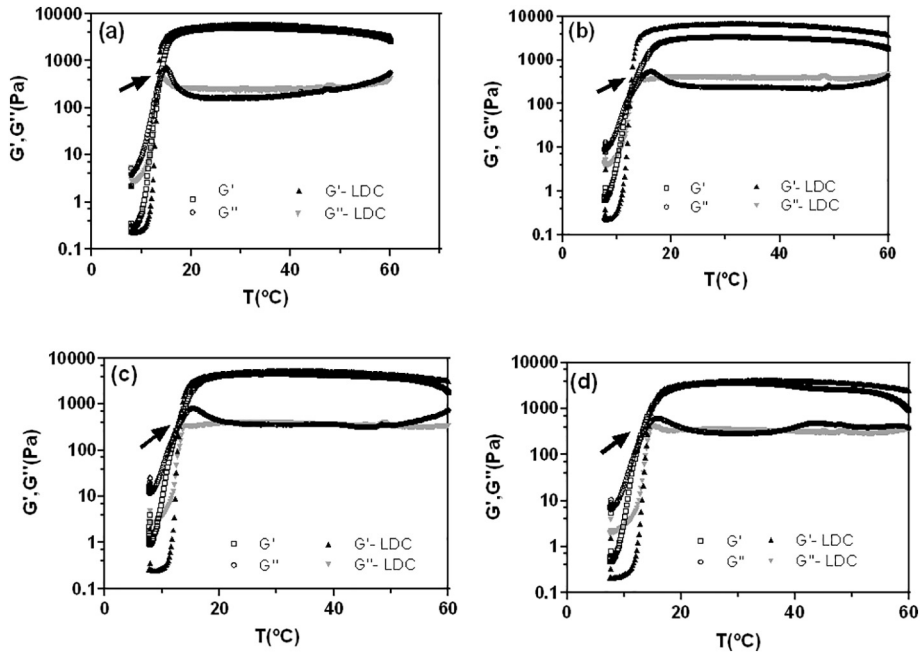

Fig. 2. Representative rheograms for organogels composed of OA-PL_{407} at 20% (a), OA-PL_{407}-LAN (0.5%, b), OA-PL_{407}-LAN (1%, c) and OA-PL_{407}-LAN (3%, d). Arrows indicate the sol-gel transition temperature.

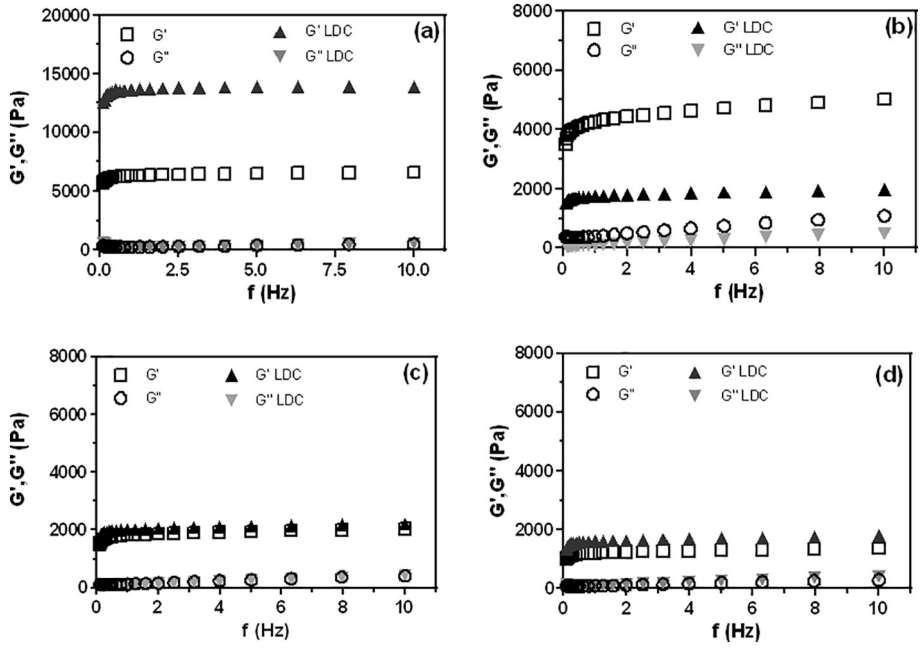

Fig. 3. Frequency sweep analysis for organogels composed of OA-PL_{407} at 20% (a), OA-PL_{407}-LAN (0.5%, b), OA-PL_{407}-LAN (1%, c) and OA-PL_{407}-LAN (3%, d).

Similar profiles were obtained after LAN incorporation into the formulations. Results showed that OA-PL_{407}-LAN (30-3) significantly reduced the LDC permeation rate compared to OA-PL_{407}, 158.7 and 182.4 $\mu g \cdot cm^{-2}$, respectively ($p < 0.01$). For OA-PL_{407} (20), LAN incorporation did not influence the amount of permeated LDC, as determined through their overlapping permeation profiles.

In general, drug flux and permeability coefficient values for OA-PL_{407} (20) were statistically different from OA-PL_{407} (30) formulations ($p < 0.001$). Furthermore, OA-PL_{407}-LAN (30-3) exhibited the lowest LDC flux and permeability coefficient values compared to OA-PL_{407} (20) and OA-PL_{407}-LAN (20-0.5; 20-1; 20-3) ($p < 0.01$) (Table 4). In contrast, similar latency times were observed for all formulations, usually close to zero. This was expected for the homogeneous artificial membrane, given that Strat-M® upper layer membranes have impregnated lipids such as ceramides, free fatty acids, cholesterol, and phospholipids (Uchida et al., 2015). In fact, some reports have suggested that Strat-M® membranes can simulate the skin barrier and should be used for predicting a drug's transdermal diffusion during the early stages of system development (Uchida et al., 2015; Simon et al., 2016; Haq et al., 2018); however, limitations in terms of transepidermal water loss have been shown to be more pronounced in Strat-M® membranes compared to skin (Carrer et al., 2018). This effect could explain the changes to ORG viscosity, modulating the drug permeation profiles. For this reason, and taking in consideration the LDC permeation profiles, flux and permeability coefficient values obtained from the ex vivo assay for OA-PL_{407} (20); OA-PL_{407} (30); OA-PL_{407}-LAN (20-3); OA-PL_{407}-LAN (30-3) were selected to evaluate the influence of PL407 concentration and LAN incorporation on LDC permeation across a skin barrier ex vivo.

As expected, LDC flux and permeability coefficients across the pig's skin were lower than the Strat-M® membrane (Table 4). Additionally, the ex vivo skin permeation studies showed different LDC profiles, where OA-PL_{407} (20), OA-PL_{407} (30), and OA-PL_{407}-LAN (20-3) exhibited high flux values while OA-PL_{407}-LAN (30-3) had significantly lower levels of permeated LDC (from ~250 to 100 $\mu g \cdot cm^{-2}$ after 8 h, $p < 0.001$) and longer lag times (~0.2 h), suggesting a possible

Table 3
Rheological parameters values of G′ (elastic) and G″ (viscous) moduli, viscosity (η*) at 25 °C and 32.5 °C and sol-gel transition temperatures (Tsol-gel) for OA-PL_{407} and OA-PL_{407}-LAN in the absence and presence of LDC.

Formulation		Additives	Tsol-gel (°C)	25 °C				32.5 °C			
				G′ (Pa)	G″ (Pa)	G′/G″	η* (×10^3, mPas·s)	G′ (Pa)	G″ (Pa)	G′/G″	η* (×10^3, mPas·s)
20%	OA-PL_{407}	–	13 ± 0.9	4889	164.2	29.8	778.5	4989	165.3	30.2	794.5
		LDC	12 ± 0.6	5670	257.6	22	903.3	5910	251.0	23.5	941.5
		Lan 0.5%	12.6 ± 1.2	3331	247	13.5	531.6	3412	244.0	14.0	544.5
		Lan 0.5% - LDC	12 ± 0.7	6541	411.3	15.9	1043	6750	405.0	16.7	1076.0
		Lan 1%	12.4 ± 1	4529	375	12	723.3	4572	366.0	12.5	730.0
		Lan 1% - LDC	12.9 ± 0.4	5089	415	12.3	812.6	5338	399.0	13.4	852.0
		Lan 3%	13.8 ± 1	3532	307	11	564.2	3593	300.0	12.0	573.9
		Lan 3% - LDC	14 ± 0.5	3833	361	10.6	612.7	4115	353.0	11.7	657.3
30%	OA-PL_{407}	–	< 8	6189	98.9	62.6	9885.2	6320	208.1	30.4	1006
		LDC		7911	105.1	75.3	1259.0	13,620	284.9	47.9	2168
		Lan 0.5%		1427	100.3	14.2	227.7	1817	119.2	15.2	289.0
		Lan 0.5% - LDC		1623	119	13.6	259.0	2017	114.7	17.6	147.5
		Lan 1%		2058	208.1	9.9	329.4	4267	392.0	10.9	681.9
		Lan 1% - LDC		967	82.6	11.7	154.5	1760	120.8	14.6	280.7
		Lan 3%		324.1	89.0	3.6	53.3	1207	82.68	14,6	192.6
		Lan 3% - LDC		8712	108.5	80	1387	13,190	183.9	71.7	256.0

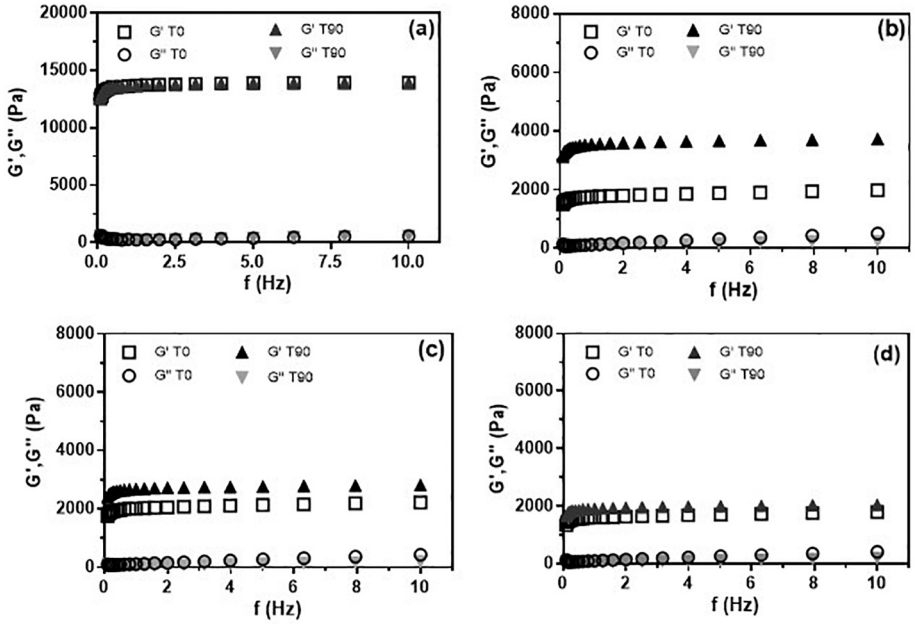

Fig. 4. Formulations stability evaluated by frequency sweep analysis (T0 and T90 refers to immediately and 90 days after preparation, respectively). Organogels composed of OA-PL$_{407}$ at 20% (a), OA-PL$_{407}$-LAN (0.5%, b), OA-PL$_{407}$-LAN (1%, c) and OA-PL$_{407}$-LAN (3%, d) containing 2% lidocaine.

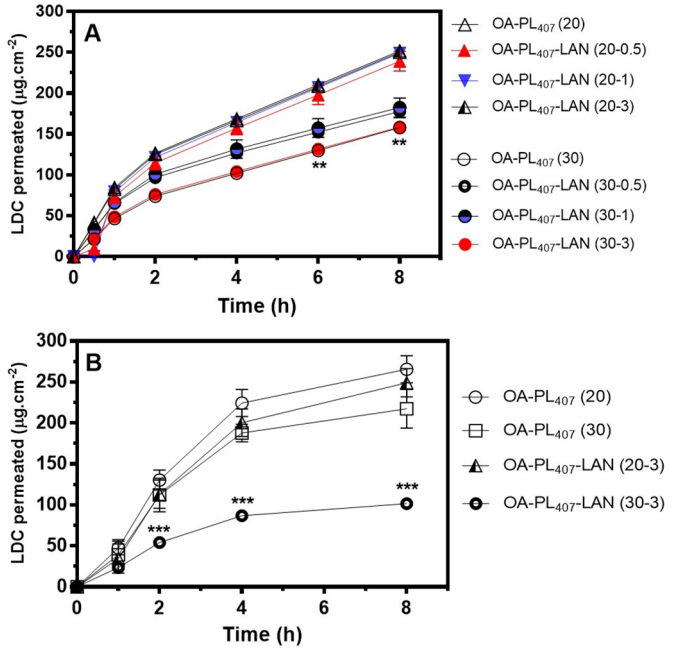

Fig. 5. Permeation profiles of lidocaine from OA-PL$_{407}$ and OA-PL$_{407}$-LAN (lanolin concentrations from 0.5 to 3%) across Strat-M® (A) and dermatomed porcine ear skin (mean ± standard deviation, n = 4–6/formulation). PL407 concentrations were 20 and 30%. Organogels formulations containing 2% of lidocaine.

retentive effect of this formulation compared to the others ORGs, despite the penetration enhancement properties of OA described in the literature (Ellaithy and El-Shaboury, 2002, Chen et al., 2018).

In this context, it is necessary to consider the influence of OA-LAN on the skin permeation of a drug. LAN has been established as an important compound capable of mimicking the stratum corneum lipid matrix (containing cholesterol, ceramides, and long chain free fatty acids), thus acting as a similar barrier to skin (Carrer et al., 2018; Sharma et al., 2018). OA has been described as an effective permeation enhancer, whereas the incorporation of highly lipophilic fatty acid mixtures, such as in LAN, does not enhance permeation (Ibrahim and Li, 2010) as observed here by the reduced LDC flux and permeation coefficient values for OA-PL$_{407}$-LAN (30–3). These effects also seem to be due to the increase on PL407 concentration, suggesting that this component may contribute to the entrapment of the organic phase (containing LDC) into the aqueous phase of the micellar matrix.

3.5. *In vitro cytotoxicity and in vivo pharmacological assays*

In vitro cytotoxicity experiments were performed to evaluate the effects of OA-PL407 (20), OA-PL407 (20-3), OA-PL407 (30) and OA-PL407 (30-3) in keratinocytes, assessed by MTT reduction. All results are presented on Fig. 6A. After cells treatment, OA-PL (20) and OA-PL407-LAN (30-3) presented the lowest cytotoxic effects, with percentages ranging from 100 to 70%, showing that the low PL407 concentration and the possible entrapment of LAN into the high concentration of aqueous phase were associated to the highest percentages of viable cells.

Pharmacological assays were used to establish the in vivo efficacy of the OA-PL$_{407}$ (20), OA-PL$_{407}$ (30), OA-PL$_{407}$-LAN (20-3), and OA-PL$_{407}$-LAN (30-3) formulations. With this animal model, the LA effects of these ORG systems were functionally compared to two commercial creams, CG and CC, which contain 2 and 4% LDC, respectively (Fig. 6A and B). After the experimental procedure, animals were observed for 24 h and no signs of skin irritancy or local toxicity were observed at the site of application.

A time course analysis showed that the percentage of animals experiencing local anesthesia after ORG application was significantly higher than observed for CG ($p < 0.001$). However, only OA-PL$_{407}$ (30) and OA-PL$_{407}$-LAN (30-3) were significantly more effective than CC ($p < 0.001$).

From the time course data, it was possible to determine the area under the efficacy curve (AUEC$_{0–6h}$) values for OA-PL$_{407}$ (20) (386.1), OA-PL$_{407}$-LAN (20-3) (400.3), OA-PL$_{407}$ (30) (450.0), and OA-PL$_{407}$-LAN (30-3) (460.0). Comparisons with CG (AUEC$_{0–6h}$ = 197.5) and CC (AUEC$_{0–6h}$ = 430) revealed statistical differences between the ORG and CG ($p < 0.001$), but no differences were observed between OA-PL$_{407}$-LAN (20-3), OA-PL$_{407}$ (30), or OA-PL$_{407}$-LAN (30-3) and CC, indicating that an enhancement of the LA effect was achieved with lower LDC

Table 4
Permeation parameters of lidocaine across artificial membrane and dermatomed porcine ear skin from OA-PL_{407} organogels.

Formulations		Strat-M®		Dermatomed skin	
		Flux ($\mu g \cdot cm^{-2} \cdot h^{-1}$)	Permeability coefficient ($cm \cdot h^{-1}$)	Flux ($\mu g \cdot cm^{-2} \cdot h^{-1}$)	Permeability coefficient ($cm \cdot h^{-1}$)
20%	OA-PL_{407}	25.8 ± 0.03	1.29 ± 0.02	23.9 ± 2.6	1.29 ± 0.14
	OA-PL_{407}-LAN 0.5	25.6 ± 0.02	1.28 ± 0.03	–	–
	OA-PL_{407}-LAN 1	25.1 ± 0.04	1.36 ± 0.03	–	–
	OA-PL_{407}-LAN 3	26.7 ± 0.04	1.33 ± 0.07	22.4 ± 2.3	1.02 ± 0.26
30%	OA-PL_{407}	16.9 ± 0.01	1.44 ± 0.03	17.1 ± 1.9	1.18 ± 0.19
	OA-PL_{407}-LAN 0.5	16.8 ± 0.07	0.84 ± 0.04	–	–
	OA-PL_{407}-LAN 1	18.3 ± 0.05	0.91 ± 0.09	–	–
	OA-PL_{407}-LAN 3	14.6 ± 0.02[a,***]	0.78 ± 0.06[a,***]	11.5 ± 1.6[a,****]	0.62 ± 0.1[a,****]

20 and 30% refer to the PL407 concentration. PL407 - poloxamer 407; LAN - lanolin; OA - oleic acid.
Data are presented as mean ± SD.
[a] Statistical differences for OA-PL_{407}-LAN 3 vs. OA-PL_{407} and OA-PL_{407}-LAN organogels.
*** $p < 0.001$.
** $p < 0.01$.

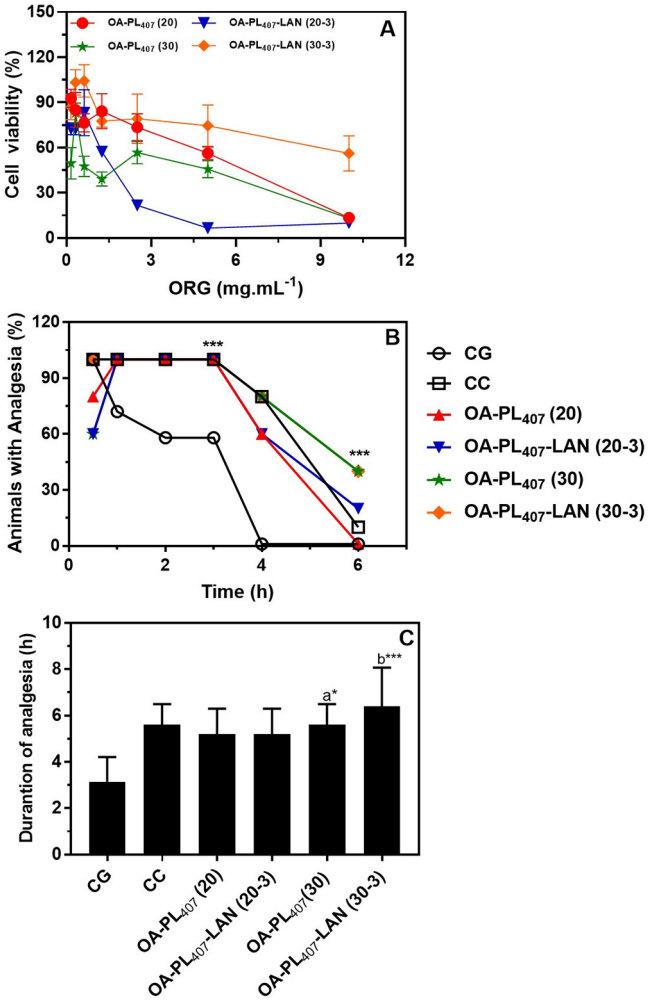

Fig. 6. Effects of ORG formulations in HaCat cells evaluated by MTT reduction test (A). Time-course (h) for animals with analgesia (%, B) and duration of analgesia (h, C) evaluated by the tail-flick test in mice after treatment with commercial formulations (Comercial gel-CG, Commercial Cream-CC, with lidocaine at 2 and 4%, respectively) and OA-PL_{407} or OA-PL_{407}-LAN. PL407 concentrations were 20 or 30% (m/v) and lanolin (LAN) concentration was 3% (m/v), (n = 5–7/group). Data expressed as mean ± standard deviation. CG vs. OA-PL_{407} (30) and b-CG vs. OA-PL_{407}-LAN (30-3). *$p < 0.05$ and ***$p < 0.001$.

concentrations using the ORG-based deliver system. Additionally, treatment with OA-PL_{407} (30) or OA-PL_{407}-LAN (30-3) extended the duration of anesthesia relative to CG ($p < 0.05$ and $p < 0.001$, respectively) (Fig. 6B).

ORGs confer some advantages over conventional systems (creams, ointments, and hydrogels) due to their high chemical stability, biocompatibility (Jatav and Ramteke, 2015; Belgamwar et al., 2008; Sagiri et al., 2013; Vintiloiu and Leroux, 2008). Their organic phase can be used as a reservoir for lipophilic molecules incorporating high drug concentrations, promoting the modulation of the permeation flux through the skin, according to adjustments on formulations composition. Also, the formation of a uniform and adherent film improves the formulation contact time with the application site (Esposito et al., 2018; Alsaab et al., 2016). All these features are essential for topical anesthesia, since the drug permeation must be controlled to avoid rapid uptake into the circulating blood, inadequate duration of action, and side effects (You et al., 2017). Importantly, despite the low flux and permeability coefficient values, OA-PL_{407}-LAN (30-3, 2% LDC) was able to permeate sufficient amounts of LDC to maintain local anesthesia for a sustained period of time, similar to CC (4% LDC). Although these are promising results, pharmacokinetic assays are in course to establish accurate correlations between therapeutic efficacy and plasma concentrations.

4. Conclusions

LDC is one of the most commonly used agents for topical anesthesia and, to date, is available in gel, cream, ointment, and bioadhesive form. However, patients frequently report inadequate analgesic effects at the site of application. Furthermore, some of these products, intended for either the skin or mucosa, require higher drug concentrations than typical topical formulations and, therefore, require additional precautions to avoid systemic toxicity. Toward overcoming these obstacles, novel pharmaceutical formulations are being developed, such as lipid-PL ORGs, that provide prolonged local anesthesia without increased risk.

In this study, we synthesized and evaluated different ORG formulations of the OA-LAN lipid mixture, chosen due to their modulating effects on skin permeation, and PL407 thermosensitive hydrogels, as the aqueous phase matrix. Both the organic and aqueous phase compositions impacted the physicochemical features, LDC percutaneous permeation profiles, and pharmacological properties. LAN incorporation increased the ΔH values compared to the PL407 hydrogels or OA-PL_{407}, in addition to evoking structural changes as determined using rheology. LAN addition to the organic phase decreased the G′/G″ ratios and also the η* values, disturbing the three-dimensional ORG network provided by the PL407 self-assembled micelles. Additionally, the OA-PL_{407}-LAN (30-3) formulation reduced the LDC flux and permeability

coefficient through skin, an effect potentially evoked by the presence of OA, LAN (3%), and PL407 (30%) in high concentrations, suggesting the enhanced entrapment capability of the organic phase (containing LDC) into the micellar aqueous phase matrix. In vivo evaluation revealed that the OA-PL_{407}-LAN systems enhanced the LA effects. Taken together, these data support the therapeutic application of this novel drug delivery system toward safely prolonging and enhancing the local anesthetic effects on skin.

Acknowledgements

This research work was supported by Coordenação de Aperfeiçoamento de Pessoal de Nível Superior (CAPES), Fundação de Amparo à Pesquisa do Estado de São Paulo (FAPESP 2014/14457-5, 2018/04036-3, 2018/02482-6), Conselho Nacional de Desenvolvimento Científico e Tecnológico (CNPq 309207/2016-9, 402838/2016-5) and UFABC Multiuser Central Facilities (CEM-UFABC). We would also like to thank Dr. Viviane Aparecida Guilherme, Gustavo Henrique Rodrigues da Silva, Paulo Sergio Castilho Preté and Marcio Aparecido Paschoal for their kind assistance.

Declarations of interest

None.

References

Akkari, A.C.S., Papini, J.Z.B., Garcia, G.K., Franco, M.K.K.D., Cavalcanti, L.P., Gasperini, A., Alkschbirs, M.I., Yokaichyia, F., de Paula, E., Tófoli, G.R., de Araujo, D.R., 2016. Poloxamer 407/188 binary thermosensitive hydrogels as delivery systems for infiltrative local anesthesia: physico-chemical characterization and pharmacological evaluation. Mater. Sci. Eng. C Mater. Biol. Appl. 68, 299–307.

Almeida, H., Amaral, M.H., Lobao, P., Lobo, J.M., 2012. Pluronic F-127 and pluronic lecithin organogel (PLO): main features and their applications in topical and transdermal administration of drugs. J. Pharm. Pharm. Sci. 15, 592–605.

Alsaab, H., Bonam, S.P., Bahl, D., Chowdhury, P., Alexander, K., Boddu, S.H., 2016. Organogels in drug delivery: a special emphasis on pluronic lecithin organogels. J. Pharm. Pharm. Sci. 19, 252–273.

Bakonyi, M., Gácsi, A., Kovács, A., Szűcs, M.B., Berkó, S., Csányi, E., 2018. Following-up skin penetration of lidocaine from different vehicles by Raman spectroscopic mapping. J. Pharm. Biomed. Anal. 154 (1–6).

Belgamwar, V.S., Pandey, M.S., Chauk, D.S., Surana, S.J., 2008. Pluronic lecithin organogel. Asian J. Pharm. Sci. 1, 134–138.

Boddu, S.H., Gupta, H., Bonam, S.P., 2014. Preclinical evaluation of a ricinoleic acid poloxamer gel system for transdermal eyelid delivery. Int. J. Pharm. 470, 158–161.

Boddu, S.H., Bonam, S.P., Jung, R., 2015. Development and characterization of a ricinoleic acid poloxamer gel system for transdermal eyelid delivery. Drug Dev. Ind. Pharm. 41, 605–612.

Carrer, V., Guzmán, B., Martí, M., Alonso, C., Coderch, L., 2018. Lanolin-based synthetic membranes as percutaneous absorption models for transdermal drug delivery. Pharmaceutics 10, E73.

Chen, L., Annaji, M., Kurapati, S., Ravis, W.R., Jayachandra Babu, R., 2018. Microemulsion and microporation effects on the genistein permeation across dermatomed duman skin. AAPS PharmSciTech. 19, 3481–3489.

Dassanayake, L.S., Kodali, D.R., Ueno, S., Sato, K., 2012. Crystallization kinetics of organogels prepared by rice bran wax and vegetable oils. J. Oleo Sci. 61, 1–9.

de Araujo, D.R., Padula, C., Cereda, C.M., Tófoli, G.R., Brito Jr., R.B., de Paula, E., Nicoli, S., Santi, P., 2010. Bioadhesive films containing benzocaine: correlation between in vitro permeation and in vivo local anesthetic effect. Pharm. Res. 27, 1677–1686.

de Araujo, D.R., da Silva, D.C., Barbosa, R.M., Franz-Montan, M., Cereda, C.M., Padula, C., Santi, P., de Paula, E., 2013. Strategies for delivering local anesthetics to the skin: focus on liposomes, solid lipid nanoparticles, hydrogels and patches. Expert Opin. Drug Deliv. 10, 1551–1563.

Dumortier, G., Grossiord, J.L., Agnely, F., Chaumeil, J.C., 2006. A review of poloxamer 407 pharmaceutical and pharmacological characteristics. Pharm. Res. 23, 2709–2728.

Ellaithy, H.M., El-Shaboury, K.M, 2002. The development of Cutina lipogels and gel microemulsion for topical administration of fluconazole. AAPS PharmSciTech 3, 77–85.

Elnaggar, Y.S., El-Refaie, W.M., El-Massik, M.A., Abdallah, O.Y., 2014. Lecithin-based nanostructured gels for skin delivery: an update on state of art and recent applications. J. Control. Release 180, 10–24.

Esposito, C.L., Kirilov, P., Roullin, V.G., 2018. Organogels, promising drug delivery systems: an update of state-of-the-art and recent applications. J. Control. Release 271, 1–20.

Haq, A., Dorrani, M., Goodyear, B., Joshi, V., Michniak-Kohn, B., 2018. Membrane properties for permeability testing: skin versus synthetic membranes. Int. J. Pharm. 539, 58–64.

Ibrahim, S.A., Li, S.K., 2010. Efficiency of fatty acids as chemical penetration enhancers: mechanisms and structure enhancement relationship. Pharm. Res. 27, 115–125.

Jantharaprapap, R., Stagni, G., 2007. Effects of penetration enhancers on in vitro permeability of meloxicam gels. Int. J. Pharm. 343, 26–33.

Jatav, M.P., Ramteke, S., 2015. Formulation and evaluation of lecithin organogel for treatment of arthritis. Int. J. Sci. World 3, 267–274.

Kaur, L., Singh, K., Paul, S., Singh, S., Singh, S., Jain, S.K., 2018. A mechanistic study to determine the structural similarities between artificial membrane Strat-M™ and biological membranes and its application to carry out skin permeation study of amphotericin B nanoformulations. AAPS PharmSciTech 19, 1606–1624.

Lee, Y., Chung, H.J., Yeo, S., Ahn, C.-H., Lee, H., Messersmith, P.B., Park, T.G., 2010. Thermo-sensitive, injectable, and tissue adhesive sol–gel transition hyaluronic acid/pluronic composite hydrogels prepared from bio-inspired catechol-thiol reaction. Soft Matter 6, 977–983.

Mady, F.M., Essa, H., El-Ammawi, T., Abdelkader, H., Hussein, A.K., 2016. Formulation and clinical evaluation of silymarin pluronic-lecithin organogels for treatment of atopic dermatitis. Drug Des. Devel. Ther. 10, 1101–1110.

Nascimento, M.H.M., Franco, M.K.K.D., Yokaichyia, F., de Paula, E., Lombello, C.B., de Araujo, D.R., 2018. Hyaluronic acid in Pluronic F-127/F-108 hydrogels for postoperative pain in arthroplasties: influence on physico-chemical properties and structural requirements for sustained drug-release. Int. J. Biol. Macromol. 111, 1245–1254.

Oshiro, A., da Silva, D.C., de Mello, J.C., de Moraes, V.W., Cavalcanti, L.P., Franco, M.K., Alkschbirs, M.I., Fraceto, L.F., Yokaichiya, F., Rodrigues, T., de Araujo, D.R., 2014. Pluronics F-127/l-81 binary hydrogels as drug-delivery systems: influence of physicochemical aspects on release kinetics and cytotoxicity. Langmuir 30, 13689–13698.

Park, K.K., Sharon, V.R.A, 2017. Review of local anesthetics: minimizing risk and side effects in cutaneous surgery. Dermatol Surg. 43, 173–187.

Patel, H.R., Patel, R.P., Patel, M.M., 2009. Poloxamers: a pharmaceutical excipients with therapeutic behaviors. Int. J. Pharm.Tech. Res. 1, 299–303.

Sagiri, S.S., Behera, B., Pal, K., Basak, P., 2013. Lanolin-based organogels as a matrix for topical drug delivery. J. Appl. Polym. Sci. 128, 3831–3839.

Sagiri, S.S., Pal, K., Basak, P., 2014. Encapsulation of animal wax-based organogels in alginate microparticles. J. Appl. Polym. Sci. 131, 1–11.

Sagiri, S.S., Kumar, U., Champaty, B., Singh, V.K., Pal, K., 2015. Thermal, electrical, and mechanical properties of tween 80/span 80-based organogels and its application in iontophoretic drug delivery. J. Appl. Polym. Sci. 132, 414–419.

Sallam, M.A., Motawaa, A.M., Mortada, S.M., 2015. An insight on human skin penetration of diflunisal: lipogel versus hydrogel microemulsion. Drug Dev. Ind. Pharm. 41, 141–147.

Sengupta, A., Behera, J., 2014. Comprehensive view on chemistry, manufacturing & applications of lanolin extracted from wool pretreatment. Am. J. Eng. Res. 3, 33–43.

Sharma, P.K., Reilly, M.J., Bhatia, S.K., Sakhitab, N., Archambault, J.D., Bhatia, S.R., 2008. Effect of pharmaceuticals on thermoreversible gelation of PEO − PPO − PEO copolymers. Colloids Surf. B: Biointerfaces 63, 229–235.

Sharma, G., Devi, N., Thakur, K., Jain, A., Katare, O.P., 2018. Lanolin-based organogel of salicylic acid: evidences of better dermatokinetic profile in imiquimod-induced keratolytic therapy in BALB/c mice model. Drug Deliv. Transl. Res. 8, 398–413.

Simon, A., Amaro, M.I., Healy, A.M., Cabral, L.M., de Sousa, V.P., 2016. Comparative evaluation of rivastigmine permeation from a transdermal system in the Franz cell using synthetic membranes and pig ear skin with in vivo-in vitro correlation. Int. J. Pharm. 512, 234–241.

Uchida, T., Kadhum, W.R., Kanai, S., Todo, H., Oshizaka, T., Sugibayashi, K., 2015. Prediction of skin permeation by chemical compounds using the artificial membrane, Strat-M (TM). Eur. J. Pharm. Sci. 67, 113–118.

Vintiloiu, A., Leroux, J.C., 2008. Organogels and their use in drug delivery–a review. J. Control. Release 125, 179–192.

Wang, J., Zhang, L., Chi, H., Wang, S., 2016. An alternative choice of lidocaine-loaded liposomes: lidocaine-loaded lipid-polymer hybrid nanoparticles for local anesthetic therapy. Drug Deliv. 23, 1254–1260.

You, P., Yuan, R., Chen, C., 2017. Design and evaluation of lidocaine- and prilocaine-coloaded nanoparticulate drug delivery systems for topical anesthetic analgesic therapy: a comparison between solid lipid nanoparticles and nanostructured lipid carriers. Drug Des. Devel. Ther. 11, 2743–2752.

Zhang, J., Michniak-Kohn, B., 2011. Investigation of microemulsion microstructures and their relationship to transdermal permeation of model drugs: ketoprofen, lidocaine, and caffeine. Int. J. Pharm. 421, 34–44.

Zhang, L., Wang, J., Chi, H., Wang, S., 2016. Local anesthetic lidocaine delivery system: chitosan and hyaluronic acid-modified layer-by-layer lipid nanoparticles. Drug Deliv. 23, 3529–3537.